Cationdiffusion in yttria-zirconia by molecular dynamics

- R.L. González-Romero[a], J.J. Meléndez[b,] D. Gómez-García[a], F.L. Cumbrera[a], A. Domínguez-Rodríguez[a], F. Wakai[c]

- [a] Departamento de Física de la Materia Condensada-ICMSE, Universidad de Sevilla-CSIC, P.O. Box 1065, 1080 Sevilla, Spain
- [b] Departamento de Física, Universidad de Extremadura, Av. de Elvas s/n., 06006 Badajoz, Spain
- [c] Secure Materials Center, Materials and Structures Laboratory, Tokyo Institute of Technology, R3-23 4259 Nagatsuta, Midori, Yokohama, 226-8503, Japan

Abstract

This paper presents a novel methodology to calculate cationdiffusion coefficients and activation energies in cubic Y2O3–ZrO2 by Molecular Dynamics. The calculation is based upon modulating the interaction potential to promote cation mobility within the lattice. The technique was calibrated by measuring static properties and oxygen self-diffusion characteristics, and then applied to cationdiffusion. The respective activation energies and diffusion coefficients agree well with experimental findings. Preliminary results about grain boundary cationdiffusion are presented for the first time as a proof of the potentiality of the procedure.

Highlights

► Novel method for Molecular Dynamics determination of diffusion coefficients. ► Cationdiffusion coefficients for cubic Y2O3–ZrO2 ceramics determined. ► Comparison with data and physical implications of the method discussed.

Keywords

Molecular Dynamics; Cationdiffusion; Yttria–zirconia ceramics

1. Introduction

Cubic yttria–zirconia ceramics (YSZ) are probably the most remarkable high ionic conductivity materials [1] and [2]. They deserve considerable attention, not only from a basic point of view but also because of their applications in fuel cells and oxygen detectors [3]. In YSZ (which has the fluorite structure, with the cations at the sites of a fcc lattice and the anions at the tetrahedral interstices), Zr4+ substitute Y3+ within the

cation sublattice, which is accompanied by the formation of one oxygen vacancy for each pair of Y3+cations to keep the electrical neutrality of the system. This elevated number of oxygen vacancies is responsible for the high ionic conductivity exhibited by YSZ.

Understanding the oxygen mobility in this system is then an essential issue. Many works have concentrated on the bulk oxygen self-diffusion in YSZ [[4], [5], [6], [7] and [8]]; although the diffusion mechanism is not fully understood yet [9], this phenomenon is already quite well characterised. A different picture concerns cationdiffusion in YSZ, which affects optical and mechanical properties. Several authors have reported values for cationdiffusion coefficients, measured either directly [[10], [11] and [12]] or from high-temperature creep or dislocation loops annealing [[13], [14], [15] and [16]] but cationdiffusion characteristics and mechanisms are far to be fully characterised and understood.

Numerical simulation has recently become a powerful tool for diffusion studies. The essential challenge for the calculation of cation diffusivities in YSZ is due to the very low probability of cation jumps in this system. To our knowledge, the only work dealing with the numerical study of cationdiffusion in YSZ is due to Kilo et al.[17]. They performed Molecular Dynamics (MD) simulations at temperatures between 2500 and 5000 K by artificially introducing Zr4+ vacancies in the equilibrium YSZ structure. Such a procedure indeed enhances cation migration, which allowed the authors to calculate diffusion coefficients and activation energies for yttrium and zirconium, but has the disadvantage to use unrealistically high number of zirconium vacancies; apart from making necessary an extrapolation to low temperatures, such a number may well alter the actual diffusion mechanism.

In this work an alternative numerical procedure for cationdiffusion analysis, inspired in the “Hyperdynamics” idea proposed by Voter [18], is described. This method does not alter the mechanism for cation migration and does not need use abnormally high temperatures; in addition, it is quite efficient in terms of computing time. The procedure has been applied to cation bulk diffusion in 8YSZ as model system, which yielded good agreement with the experimental findings. In addition, consistent calculations of grain boundary cationdiffusion coefficients are performed by the first time. The results are relevant because the ability to control cationdiffusion characteristics may help in the application-specific design of YSZ-based materials.

2. Numerical procedure

2.1. Calculation setup

MD simulations have been performed on a 8 mol% YSZ model system by the LAMMPS code [19], using a simulation box of 5 × 5 × 5 YSZ unit cells and periodic boundary conditions. For 8YSZ, the exact number of zirconium cations were replaced by yttrium ones, and the proper number of oxygen vacancies were introduced to keep the electroneutrality of the system, giving 426 Zr4+, 74 Y3+ and 963 O2− ions; all the substitutions were randomly made. Since the diffusion features may be dependent on the particular positions of the dopant cations, five different random configurations were considered; the diffusion coefficients and activation energies reported here were taken as the average over this five samples population. For grain-boundary diffusion, a bicrystal model containing a Σ5 grain boundary was built following a previous work [20] (cf. Fig. 1); this grain boundary was chosen because it has been extensively studied in the past. In this case, the size of the simulation cell was 6.424 nm × 2.409 nm × 2.032 nm, with the longer dimension perpendicular to the plane of the grain boundary; these dimensions were chosen so as to be 8 times the Σ5 coincidence site lattice (CSL) unit cell length in the plane perpendicular to the grain boundary and 3 times this CSL length and 4 times the fluorite unit cell length along the axes parallel to the grain boundary. Each grain contained 398 Zr4+, 70 Y3+ and 901 O2− ions. Again, five different configurations were considered for statistical significance.

The interaction between atoms i and j was modelled by a Buckingham potential coupled with a long-range Coulombic term:

$$V_{ij}(r) = A_{ij}\exp\left(-\frac{rij}{\rho}\right) - \frac{C_{ij}}{r_{ij}^6} + \frac{1}{4\pi\varepsilon_0}\frac{q_i q_j}{r_{ij}}$$

(1)where rij is the distance between atoms i and J, qi holds for the charge of atom i and ε0 is the dielectric constant. Parameters Aij, ρ and Cij were taken from the literature [21] and listed in Table 1.

Each initial configuration was optimised by energy minimization followed by a short run (10 ps) of MD under NVE conditions at T = 0 K. After this, a temperature in the range 1500 K–3000 K was set; this is the usual range in diffusion experiments in YSZ and is low enough for the concentrations of complex defects and cation vacancies to be negligible. After raising the temperature and stabilising the system, MD runs were made for 200 ps in the NPT ensemble, with the pressure of the system at each temperature taken as:

$$p(T) = p_0 + \frac{Nk_BT}{V_0}$$

(2)where N is the number of atoms of the system, kB Boltzmann's constant and p0 and V0 the pressure and volume of each minimised supercell.

The mean square displacement (msd) < r2 > of each ion species was then computed as a function of the simulation time t, from which the diffusion coefficient was calculated according to the Nernst–Einstein formula [22]:

$$D = \lim_{t\to\infty} \frac{r^2}{6t}.$$

For bulk diffusion, all the ions of the same species within the simulation cells were taken in the calculation of the msd. For grain-boundary diffusion only ions within 6 nm at each side of the grain boundary were considered for the calculation of the msd.

2.2. Description of the method

Without additional hypotheses, the potential given by Eq. (1) gives rise to negligible msd for cations, and therefore diffusivities virtually equal to zero. To overcome this difficulty, we multiplied the whole interaction potential by a factor a < 1. The deliberate weakening of the atomic bonds was expected to increase the jump probability for cations, which is the key point of the alternative method presented here. In our case, only values α ≤ 0.2 were actually used, since no cation movement was apparent for higher values of α.

The cation diffusion coefficient then results to depend on α as follows [22]:

$$D(\alpha, T) = D_0 \alpha^{0.44} \exp\left(-\frac{Q(\alpha)}{k_B T}\right)$$

where a(α) is a typical jump length (which may be taken in first approximation as the lattice parameter), ω(α) is the attempt frequency (of the order of the Debye frequency) and Q(α) holds for the activation energy for cationdiffusion. Test simulations showed the lattice parameter of the system to vary as a ∝ α− p, with p ≈ 0.03. On the other hand, a calculation within the harmonic approximation shows that the normal frequencies of the system must be proportional to α1/2. Eq. (4) then reduces to:

$$D(T) = D(\alpha_0, T)\alpha_0^{-0.44} \exp\left(=\frac{Q-Q(\alpha_0)}{k_B T}\right)$$

where D0 is independent on α. Eq. (5) constitutes the basis for the calculations within this work. Indeed, the activation energy at given α0 may be calculated from diffusion coefficients taken at different temperatures from an Arrhenius plot; the slope of the best-fit straight line is proportional to Q(α0), and extrapolation to α = 1 gives the actual activation energy Q. On the other hand, the diffusion coefficient at a given temperature may be calculated by taking α = 1 in Eq. (5), which yields:

$$D = \phi \Gamma a^2$$

where D(α0, T) is the diffusion coefficient calculated from Eq. (5) at a reference α0 value.

3. Results

The reliability of the proposed methodology was primarily checked out by recovering some static properties of 8YSZ. For instance, the energy per atom of the system ε was found to vary linearly with α; the actual energy was ε(a = 1) = − 35.655 ± 0.009 eV, which correlates fairly well with data reported elsewhere [23] and [24]. In addition, we focused on the lattice parameter. As was pointed out before, calculations performed varying α at given temperatures should give rise to the function a(α), whose extrapolation to α = 1 yields the actual lattice parameter of the system. Fig. 2 depicts the lattice parameters obtained from our simulations, which are again in good agreement with MD calculations [25] and experimental data [26].

Subsequently, the validity of our treatment was investigated by applying it to oxygen bulk diffusion. Fig. 3 and Fig. 4 display the activation energy vs. α and diffusion coefficient vs. T− 1 for oxygen bulk self-diffusion, respectively. The activation energy fits reasonably to a lineal function of α; extrapolation to α = 1 yielded Qb(oxygen) = 0.89 ± 0.07 eV, which correlates with experiments, simulation data and first-principles calculations reported elsewhere for similar temperature conditions [[9], [11], [23], [25], [27], [28], [29], [30], [31], [32] and [33]]; Table 2 contains a summary of the published data. Analogously the diffusion coefficients shown in Fig. 4 are in good agreement with experimental data to within one order of magnitude, which is typical in the measurement of diffusion coefficients in oxide solids (cf. Fig. 5). All these tests were satisfactory proofs of the validity of our proposed methodology.

Fig. 3 shows the Q(α) functions for bulk diffusion of zirconium and yttrium as well. Calculations could be performed up to α ≈ 0.18 before the mean square displacements fell to be undetectable. In both cases the data could be reasonably fitted to straight lines. Extrapolation to α = 1 yielded virtually the same activation energy for both cation species: Qb(cations) = 2.6 ± 0.1 eV. The zirconium and yttrium diffusion coefficients are included in Fig. 4. It must be remarked that, in all cases, the characteristics of yttrium diffusion (energies and diffusion coefficients) were less accurately calculated than those for zirconium; essentially, this is due to the fact that the number of yttrium cations is much lower than that of zirconium ones, which results in less defined averages. That is probably the reason why we do not get yttrium diffusion coefficients which are higher than those for zirconium. We postpone the comparison of the calculated data with experimental ones to the discussion section below.

Our methodology was finally applied to the study of grain-boundary diffusion in a bicrystal model comprising the Σ5 grain boundary drafted in Fig. 1. Fig. 6 shows the

activation energies vs. α functions for grain boundary diffusion of oxygen (a), zirconium (b) and yttrium (c); in Fig. 7 the corresponding diffusion coefficients are plotted vs. T1. Oxygen grain boundary self-diffusion characteristics have been rarely reported in the literature; however, experimental and simulation studies have revealed that it ranges from 1.08 to around 1.20 eV [[34], [35], [36], [37] and [38]], in close agreement with the data reported here. Regarding the values for cationdiffusion, these are actually the first reported ones calculated by Molecular Dynamics in the YSZ system, to the authors' best knowledge.

4. Discussion

The numerical study of cationdiffusion in YSZ is handicapped because of the extremely low jump probability exhibited by Zr4+ and Y3+cations which, in turn, may be ascribed to the high formation enthalpy of cation vacancies (which is estimated to be around 2.8 eV [39]); this means that the fraction of cation vacancies in our system at 2000 K is of the order of 10−7, that is, virtually zero. In a recent paper, Kilo et al. [17] have overcome this handicap by conveniently handling the model system. First, they have artificially introduced well-defined concentrations of cation vacancies higher than those expectable by the formation enthalpies; secondly, they have used high temperatures (between 2700 K and 5000 K, approximately). In those conditions, the jump probability for cations greatly increases, and diffusion parameters (activation energy and diffusion coefficient) may be calculated; extrapolation to the actual concentration of vacancies and temperatures gives activation energies and diffusivities which agree well with experimental data. We are presenting here an alternative methodology to calculate cationdiffusion coefficients and activation energies by MD which does not require using artificial vacancies concentrations or extremely high temperatures. In addition, it is fully consistent with the well-studied oxygen diffusion and does not seem to show any physical incongruence. Another point favouring our methodology is its relative cheapness in computing time.

Despite its success, some points remain unclear in Kilo and co-worker's procedure. One of them is the role played by the unrealistic concentration of cation vacancies employed. Indeed, the authors admit that their diffusion coefficients are much higher than the experimental ones extrapolated to high vacancies concentrations; in addition, they find that these coefficients are barely dependent on the content of yttrium, in contradiction with the experimental findings [12]. In our opinion, these trends arise because the diffusion mechanism is altered by the high concentration of cation vacancies; this induces a strong correlation between successive cation jumps which affects diffusion[9]. On the other hand, Kilo et al.'s calculations yielded apparent activation energy close to 4.4 eV for 8YSZ. This value made them justify an

exceptionally low value for the formation enthalpy of cation vacancies, contrary to the experimental evidence.

Let us consider this point with a greater detail. From a microscopic point of view, diffusion arises as a consequence of the individual movement of diffusing species through discrete jumps at available lattice sites. In a general sense, the diffusion coefficient may be written as

$D=\phi\Gamma a^2$

where Γ is the average number of atomic jumps per unit time, a is the jump length (of the order of the atomic parameter) and φ is a geometric factor which depends on the particular crystal structure. The number of jumps Γ may be written as

$\Gamma=\xi\gamma$

where ξ depends on the number of sites available for the diffusing species to jump and γ is the jumping frequency. For diffusion mediated by vacancies, ξ is proportional to the concentration of vacancies, which depends on the temperature through an Arrhenius-type law:

$$\gamma \propto \exp\left(-\frac{\Delta g_m}{k_B T}\right)$$

with Δgf holding for the free enthalpy per atom for vacancies formation. The atomic jumping process is also thermally activated, so that the frequency γ may be written as:

$$Q = \Delta g_f + \Delta g_m.$$

being Δgm the free enthalpy per atom for migration of the diffusing species. The overall dependence of the diffusion coefficient on the temperature is then described by the effective activation energy:

$Q=\Delta gf+\Delta gm$.

A third term may appear if the concentration of defects is high enough that they associate to form complex defects; given the small concentrations appearing in our system, we will neglect such a possibility in what follows.

Eq. (11) indicates that, if the number of available sites for atomic jumps is an exponentially growing function of temperature, then both migration and formation free enthalpies must be taken into account when one calculates the activation energy. This is the situation in experimental measurements of diffusion, which yield apparent activation energies of the form (11). The situation in MD simulations is not the same; these are performed at given number of particles, so that the formation term Δgf is

not calculated. In other words, MD only estimates the free enthalpy for migration, but not the total activation energy for diffusion.

With this in mind, let us consider then the MD simulation of oxygen diffusion, where the number of oxygen vacancies is strictly constant at all the temperatures. Simulations then mimics reality, since in YSZ the concentration of oxygen vacancies is univocally determined by the amount of dopant cations added during sintering, much higher than the thermally activated concentration. Therefore, the activation energy for oxygen diffusion is completely determined by oxygen migration, and no formation contribution has to be added; simulations and experiments may be directly compared in this case. One finds something different for MD simulation of cationdiffusion however. Now the number of cation vacancies is zero. According to the previous statement, MD simulations entail only atom migration, and it is the migration energy for cationdiffusion what one calculates; in order to get the actual activation energy (and therefore to compare with experiments), one must add the corresponding formation enthalpy.

The activation (migration) energy for diffusion calculated here depends linearly on the modulation parameter α. This behaviour can be understood by considering that:

$\Delta g_m = \Delta h_m - T\Delta s_m$

where Δhm and Δsm denote enthalpy and entropy of migration per atom, respectively. The Δhm term is linear in α, which can be understood from the way in which we have handled the interaction potential. The Δsm term is much more difficult to estimate however. According to Vineyard [40], the migration entropy arises from the change in lattice vibration frequencies associated to the displacement of the jumping atom from its equilibrium configuration. Within the harmonic approximation, it is given by:

$$\Delta s_m = k_B ln\left[\frac{\Pi_{i=1}^{3N}\omega_i^{(0)}}{\omega_0 \Pi_{i=1}^{3N-1}\omega_i^{(s)}}\right]$$

where {ω(0)} and {ω(s)} are respectively the normal frequencies of the system when the diffusing atom locates close the energy minimum (i.e., close to its equilibrium position) and at the saddle point between two equilibrium positions; ω0 is the frequency of vibration of the diffusing atom along the diffusion path. From Eq. (13) it is clear that the migration entropy should not show any dependence on α, since the dependences cancel exactly in the numerator and the denominator of the term within brackets. The trends shown by our data seem then to be reasonable from the physical point of view.

We are now in conditions to compare our simulation data with experiments. Experimental values for the activation energies for cationdiffusion range between 4.4 eV and 5.3 eV [10], [12], [15], [16] and [41]. As described above, all the experimental

activation energies contain the term for the enthalpy of formation of cation vacancies. From dislocation annealing, Chien and Heuer estimated the enthalpy of formation of different types of cluster of vacancies to be around 2.8 eV [15]. Accepting that the enthalpy of formation is similar for cation vacancies, experimental data indicate that the enthalpy of migration for cationdiffusion should range between 1.6 eV and 2.5 eV. In rigour, these energies account for migration mediated by vacancies. However, since the concentration of these defects is extremely low at the high temperatures considered, it can be accepted that the migration energies are not affected much by their presence; in such a case the previous estimations can be then directly compared to our experimental results. Fig. 8 shows a comparison between the values obtained within this work (properly corrected by the formation free enthalpy term) and experimental and calculated data reported elsewhere. The agreement is acceptable to within one order of magnitude.

Of course, several questions remain unconsidered. For instance, it is not clear to us yet if our method can account for the diffusion mechanism in YSZ. In addition, future research should include the study of the surface effects, which is a key fact for the comprehension of plasticity at the nanoscale [42] and [43].

Acknowledgements

The authors wish to acknowledge financial support by the Spanish “Ministerio de Ciencia e Innovación” through the projects MAT2009-14351-C02-01 and MAT2009-14351-C02-02. RLGR also acknowledges financial support by the Spanish “Agencia Española de Cooperación Internacional y Desarrollo” (AECID) through grant no. 536875. DGG wishes to acknowledge the funding awarded by the Japan Society for the Promotion of Science (JSPS) during his sabbatical stays in Tokyo Institute of Technology (2005, 2006 and 2009). FW and DGG also acknowledge the financial support by the Materials and Structure Lab at Tokyo Institute of Technology through the Joint Project settled down between this institution and the University of Seville.

References

[1] V.S. Stubican, G.S. Corman, J.R. Hellman, G. Senft , N. Claussen, M. Rühle, A.H. Heuer (Eds.), Science and Technology of Zirconia 2, The American Ceramic Society, Columbus, OH (1983)

[2] J.A. Kilner, R.J. Brooks

Solid State Ionics, 6 (1982), p. 237

[3] S.C. Singhal

Solid State Ionics, 152–153 (2002), p. 405

[4] K. Park, D.R. Olander

J. Electrochem. Soc., 138 (1991), p. 1154

[5] P.S. Manning, J.D. Sirman, R.A. De Souza, J.A. Kilner

Solid State Ionics, 100 (1997), p. 1

[6] P.S. Manning, J.D. Sirman, J.A. Kilner

Solid State Ionics, 93 (1996), p. 125

[7] T. Suemoto, M. Ishigame

Solid State Ionics, 21 (1986), p. 225

[8] V.V. Kharton, F.M.B. Marques, A. Atkinson

Solid State Ionics, 174 (2004), p. 135

[9] R. Krishnamurthy, Y.-G. Yoon, D.J. Srolovitz, R. Car

J. Am. Ceram. Soc., 87 (2004), p. 1821

[10] Y. Oishi, K. Ando, Y. Sakka, M.F. Yan, A.H. Heuer (Eds.), Additives and Interfaces in Electronic Ceramics, The American Ceramic Society, Columbus, OH (1983), pp. 207–218

[11] H. Solmon, J. Chaumont, C. Dolin, C. Monty

Ceram. Trans., 24 (1991), p. 175

[12] M. Kilo, G. Borchardt, B. Lesage, O. Kaïtasov, S. Weber, S. Scherrer

J. Eur. Ceram. Soc., 20 (2000), p. 2069

[13] D. Dimos, D.L. Kohlstedt

J. Am. Ceram. Soc., 70 (1987), p. 531

[14] D. Gómez-García, J. Martínez-Fernández, A. Domínguez-Rodríguez, J. Castaing

J. Am. Ceram. Soc., 80 (1997), p. 1668

[15] F.R. Chien, A.H. Heuer

Phil. Mag. A, 73 (1996), p. 681

[16] A. Domínguez-Rodríguez, A.H. Heuer, J. Castaing

Rad. Eff. & Def. Solids, 119–121 (1991), p. 759

[17]M. Kilo, M.A. Taylor, C. Argirusis, G. Borchardt, R.A. Jackson, O. Schulz, M. Martin, M. Weller

Solid State Ionics, 175 (2004), p. 823

[18] A.F. Voter

Phys. Rev. Lett., 78 (1997), p. 3908

[19] S. Plimpton

J. Comp. Phys., 117 (1995), p. 1

[20] T. Oyama, M. Yoshiya, H. Matsubara, K. Matsunaga

Phys. Rev. B, 71 (2005), p. 224105

[21] M.O. Zacate, L. Minervini, D.J. Bradfield, R.W. Grimes, K.E. Sickafus

Solid State Ionics, 128 (2000), p. 243

[22] H. Mehrer

Diffusion in Solids, Springer Verlag, Berlin (2007)

[23] P.K. Schelling, S.R. Phillpot, D. Wolf

J. Am. Ceram. Soc., 84 (2001), p. 1609

[24] X. Li, B. Hafskjold

J. Phys. Condens. Matter, 7 (1995), p. 1255

[25] W. Araki, Y. Arai

Solid State Ionics, 181 (2010), p. 1534

[26] M. Biswas, C.S. Kumbhar, D.S. Gaoutam, ISRN Nanotechnology (2011) 305687.

[27]A.I. Ioffe, D.S. Rutman, S.V. Karpachov

Electrochim. Acta, 23 (1978), p. 141

[28] R. Pornprasertsuk, P. Ramanarayanan, C.B. Musgrave, F.B. Prinz

J. Appl. Phys., 98 (2005), p. 103513

[29] C. Zhang, C.-J. Li, G. Zhang, X.-J. Ning, C.-X. Li, H. Liao, C. Coddet

Mat. Sci. Eng. B, 137 (2007), p. 24

[30] C.-C.T. Yang, W.-C.J. Wei, A. Roosen

Mater. Chem. Phys., 81 (2003), p. 134

[31] T. Arima, K. Fukuyo, K. Idemitsu, Y. Inagaki

J. Mol. Liq., 113 (2004), p. 67

[32] Y. Oishi, K. Ando

Transport in Nonstroichiometric Compounds, Plenum Press, New York (1983)

[33] N. Sawaguchi, H. Ogawa

Solid State Ionics, 128 (2000), p. 183

[34] X. Guo, J. Maier

J. Electrochem. Soc., 148 (2001), p. E121

[35] S.P.S. Badwal

Solid State Ionics, 76 (1995), p. 67

[36] S.P.S. Badwal, J. Drennan

Solid State Ionics, 40–41 (1990), p. 869

[37] S.P.S. Badwal, S. Rajendran

Solid State Ionics, 70–71 (1994), p. 83

[38] R.L. González-Romero, J.J. Meléndez, D. Gómez-García, F.L. Cumbrera, A. Domínguez-Rodríguez, to be published (2011).

[39] F.R. Chien, A.H. Heuer

Phil. Mag., A73 (1996), p. 681

[40] G.H. Vineyard

J. Phys. Chem. Solids, 3 (1957), p. 121

[41] M. Kilo, M.A. Taylor, C. Argirusis, G. Borchardt, B. Lesage, B. Weber, S. Scherrer, H. Scherrer, M. Schroeder, M. Martin

J. Appl. Phys., 94 (2003), p. 7547

[42] D. Gómez-García, C. Lorenzo-Martín, A. Muñoz-Bernabé, A. Domínguez-Rodríguez

Phys. Rev. B, 67 (2003), p. 144101

[43] D. Gómez-García, E. Zapata-Solvas, A. Domínguez-Rodríguez, L. Kubin

Phys. Rev. B, 80 (2009), p. 214107

[44] A. Dwivedi, A.N. Cormack

Phil. Mag., 61 (1990), p. 1

[45] H.W. Brinkman, W.J. Briels, H. Verweij

Chem. Phys. Lett., 247 (1995), p. 386

Figure captions

Figure 1. Model bicrystal with a Σ5 grain boundary (from Ref. [20]). Some relevant crystallographic directions are included for clarity. Black, white and grey balls represent yttrium, zirconium and oxygen, respectively.

Figure 2. Variation of the calculated lattice parameter of 8YSZ with temperature. Data taken from the literature are included for comparison.

Figure 3. Q(α) functions calculated for oxygen, zirconium and yttrium bulk diffusion in 8YSZ. The activation energies reported are those extrapolated to α = 1 from the best-fit straight lines.

Figure 4. Arrhenius plot for oxygen, zirconium and yttrium bulk diffusion coefficients calculated from Eq. (6)

Figure 5. Comparison of the oxygen bulk self-diffusion coefficients calculated within this work with experimental and simulation data taken from the literature.

Figure 6. Q(α) functions calculated for oxygen (a), zirconium (b) and yttrium (c) bulk and Σ5 grain boundary diffusion. The reported activation energies are the extrapolations to α = 1 made from the best-fit straight lines (shown).

Figure 7. Diffusion coefficients for oxygen, zirconium and yttrium diffusion along the Σ5 grain boundary, calculated from Eq. (6).

Figure 8. Comparison of the cation bulk diffusion coefficients in YSZ calculated within this work with experimental and simulation data reported elsewhere. The calculated coefficients have been corrected by the proper free enthalpy of cation vacancy formation.

Table 1

Table 1. Potential parameters for YSZ used in this study

Ion pair	***Aij* (eV)**	***ρij* (Å)**	***Cij* (eV Å^6)**
O^{2-}–O^{2-}	9547.96	0.2192	32.0
Zr^{4+}–O^{2-}	1502.11	0.3477	5.1
Y^{3+}–O^{2-}	1766.40	0.33849	19.43

From Ref. [21].

Table 2

Table 2. Summary of experimental and calculated data for the activation energy of oxygen bulk diffusion.

Composition	**Method**[a]	**Model**	**Potential**	**Temperature range (K)**	**Activation energy (eV)**	**Reference**
8YSZ	MD	3 × 3 × 3 unit cells NPT	Brinkman et al. [45]	1000–2000	0.80	[31]
8YSZ	MD	5 × 5 × 5 unit cells NPT, 0.1 MPa	Dwivedi and Cormack [44]	300–1500	0.79	[33]
8YSZ	KMC	50 × 50 × 50 unit cells	–	1000–2200	0.60	[9]
8.3YSZ	KMC	5 × 5 × 5 unit cells	–	600–1500	0.70	[28]
9.5YSZ	OTD	$^{18}O/^{16}O$ isotope exchange	–	723–923	0.91	[5]
				923–1373	0.82	
	IS	10 Hz–13 MHz 50 mV		523–1073	1.10	
9.5YSZ	OTD	$^{18}O/^{16}O$ isotope exchange	–	573–1273	0.88–1.10	[11]

a MD — Molecular Dynamics; KMC — Kinetic Monte Carlo; OTD — oxygen tracer diffusion; IS — AC impedance spectroscopy; SIMS — secondary ion mass spectrometry.

Figure 1

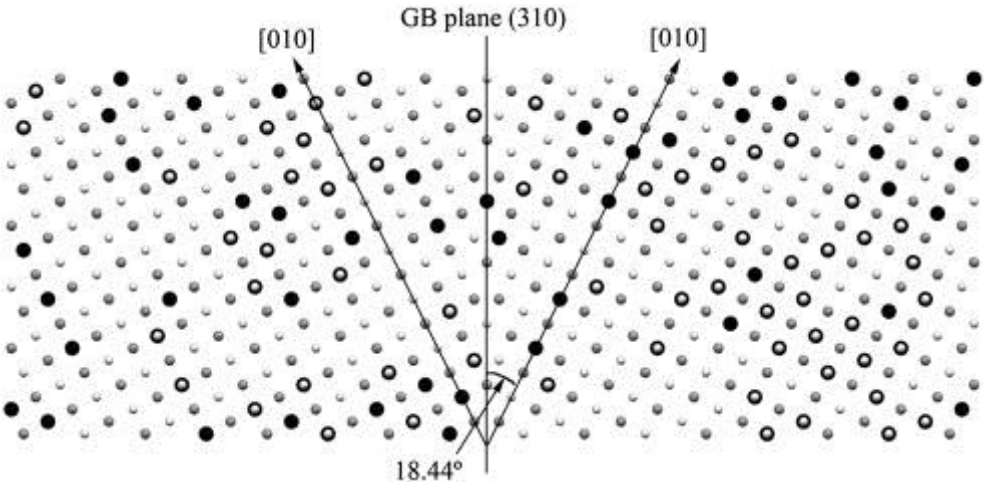

Figure 2

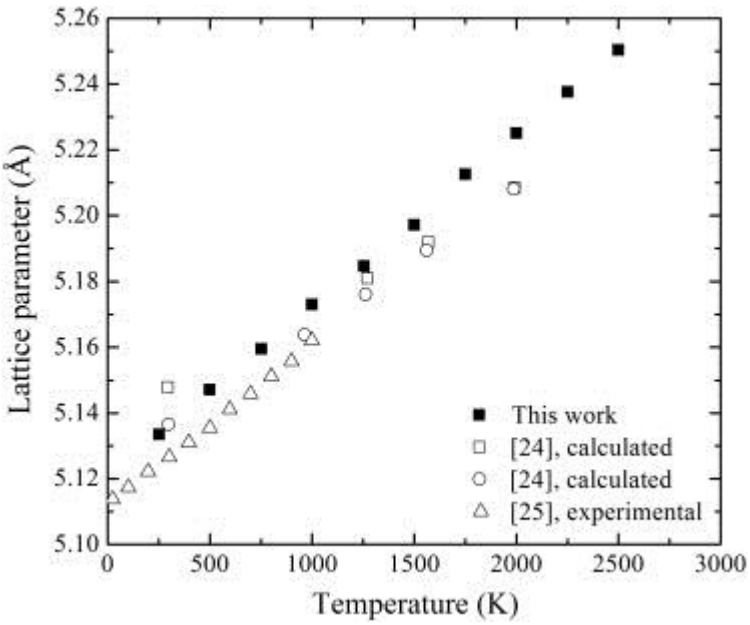
Lattice parameter (Å)
Temperature (K)
5.10
5.12
5.14
5.16
5.18
5.20
5.22
5.24
5.26
0
500
1000
1500
2000
2500
3000
This work
[24], calculated
[24], calculated
[25], experimental

Figure 3

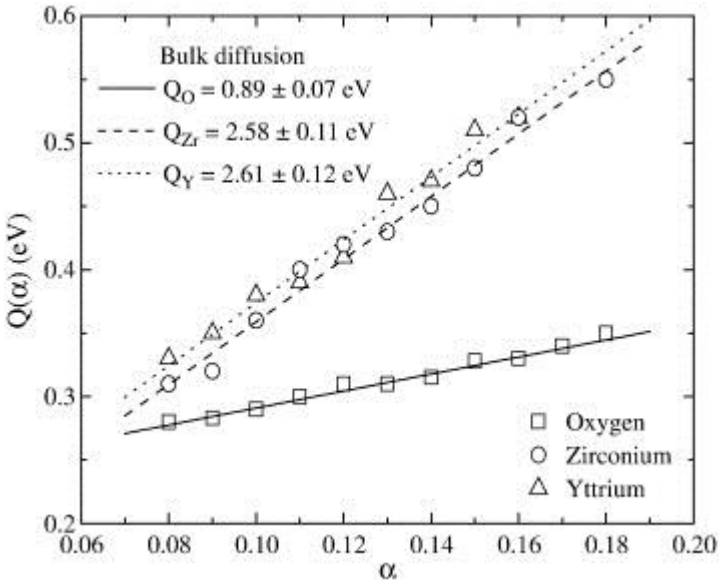
Bulk diffusion
$Q_O = 0.89 \pm 0.07$ eV
$Q_{Zr} = 2.58 \pm 0.11$ eV
$Q_Y = 2.61 \pm 0.12$ eV
Oxygen
Zirconium
Yttrium
Q(α) (eV)
α
0.2
0.3
0.4
0.5
0.6
0.06
0.08
0.10
0.12
0.14
0.16
0.18
0.20

Figure 4

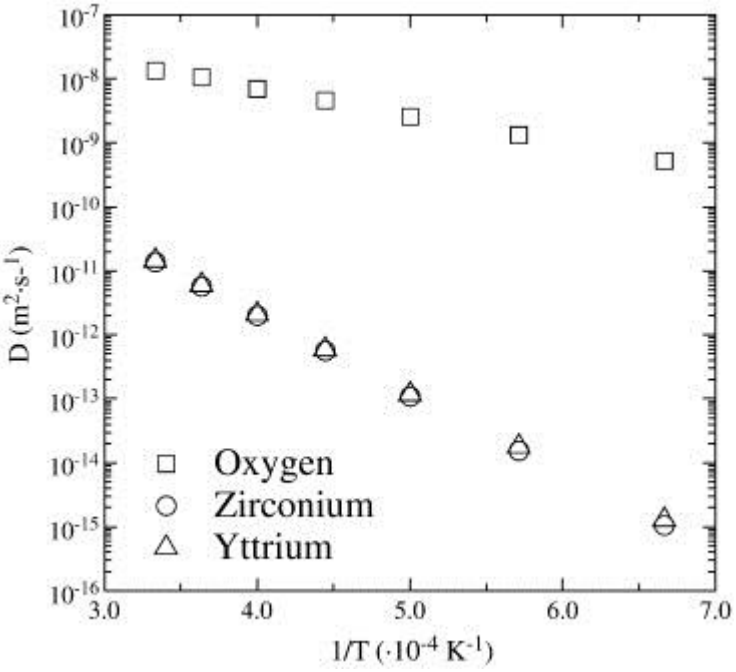
D (m²·s⁻¹)
10⁻⁷
10⁻⁸
10⁻⁹
10⁻¹⁰
10⁻¹¹
10⁻¹²
10⁻¹³
10⁻¹⁴
10⁻¹⁵
10⁻¹⁶
3.0
4.0
5.0
6.0
7.0
1/T (·10⁻⁴ K⁻¹)
Oxygen
Zirconium
Yttrium

Figure 5

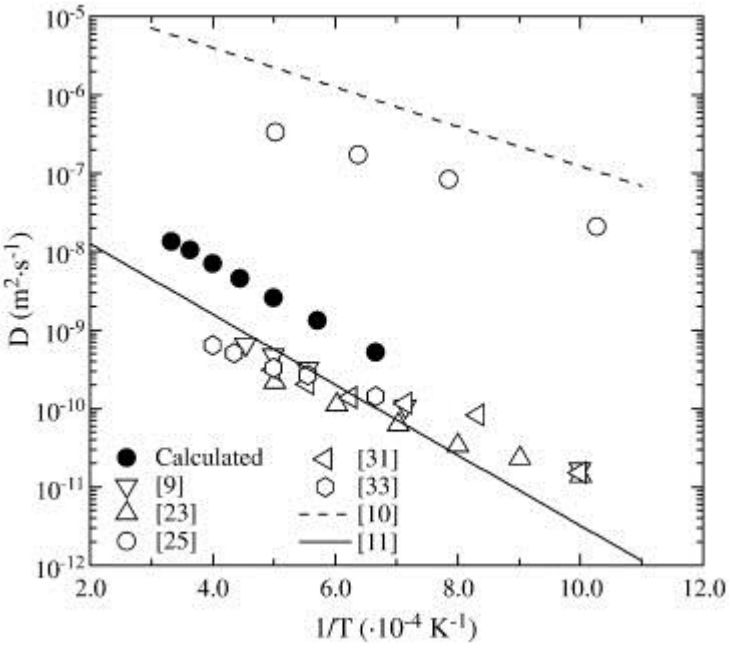

Figure 6

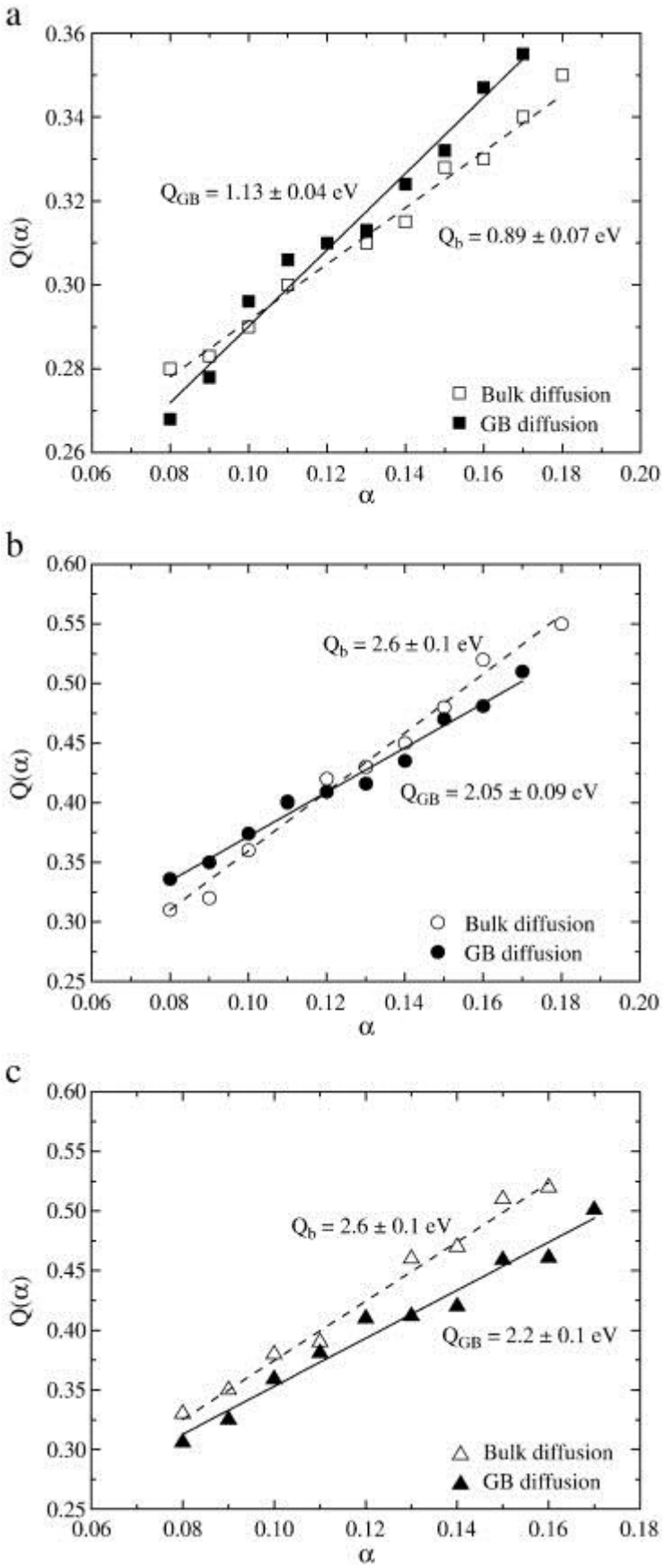
a
Q(α)
α
Q_{GB} = 1.13 ± 0.04 eV
Q_b = 0.89 ± 0.07 eV
Bulk diffusion
GB diffusion
b
Q(α)
α
Q_b = 2.6 ± 0.1 eV
Q_{GB} = 2.05 ± 0.09 eV
Bulk diffusion
GB diffusion
c
Q(α)
α
Q_b = 2.6 ± 0.1 eV
Q_{GB} = 2.2 ± 0.1 eV
Bulk diffusion
GB diffusion

Figure 7

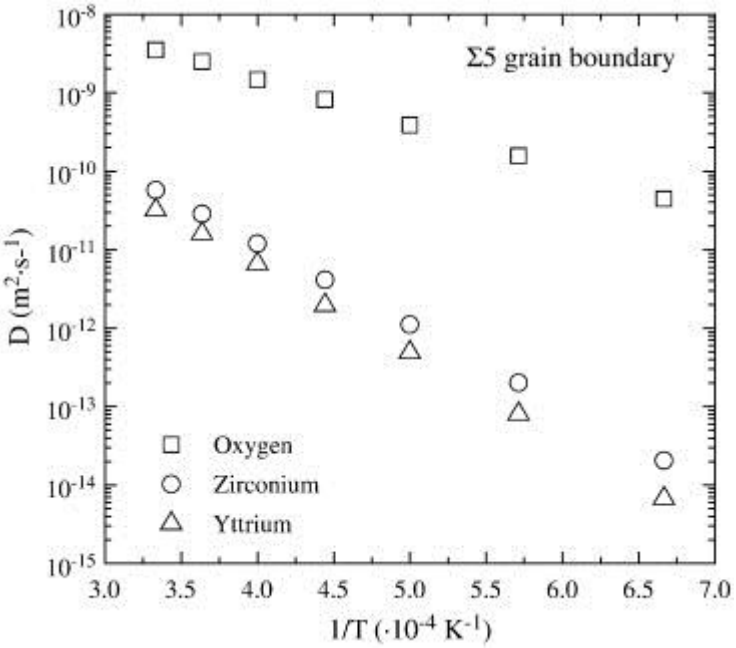
Σ5 grain boundary
Oxygen
Zirconium
Yttrium
D (m²·s⁻¹)
1/T (·10⁻⁴ K⁻¹)
10⁻⁸
10⁻⁹
10⁻¹⁰
10⁻¹¹
10⁻¹²
10⁻¹³
10⁻¹⁴
10⁻¹⁵
3.0
3.5
4.0
4.5
5.0
5.5
6.0
6.5
7.0

Figure 8

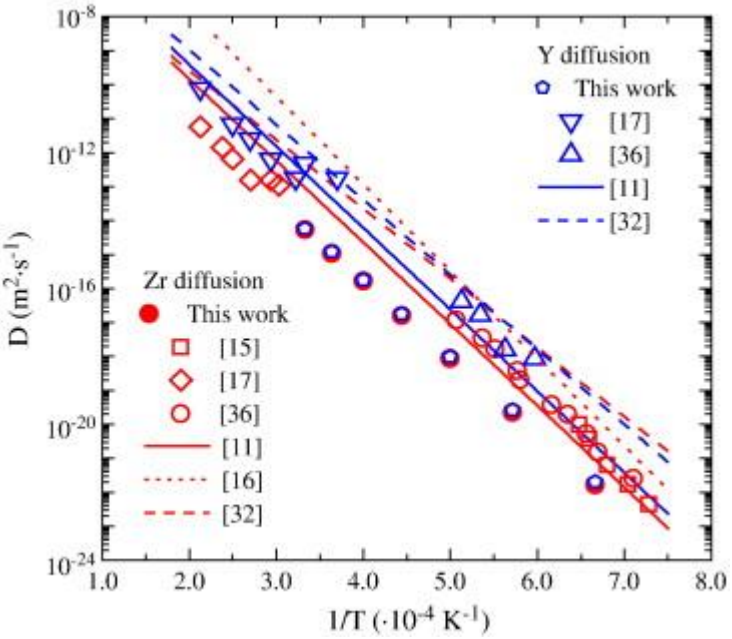
Y diffusion
This work
[17]
[36]
[11]
[32]
Zr diffusion
This work
[15]
[17]
[36]
[11]
[16]
[32]
D (m²·s⁻¹)
1/T (·10⁻⁴ K⁻¹)
10⁻⁸
10⁻¹²
10⁻¹⁶
10⁻²⁰
10⁻²⁴
1.0
2.0
3.0
4.0
5.0
6.0
7.0
8.0